Vol. 18, No. 1 (2019) 251-271
Revista Mexicana de Ingeniería Química

PREPARATION AND DEGRADATION STUDY OF HDPE/PLA POLYMER BLENDS FOR PACKAGING APPLICATIONS

ESTUDIO DE OBTENCIÓN Y DEGRADACIÓN DE MEZCLAS POLIMÉRICAS DE PEAD/APL PARA APLICACIONES DE EMBALAJE

A.M. Torres-Huerta[1]*, M.A. Domínguez-Crespo[1], D. Palma-Ramírez[2], A.I. Flores-Vela[3], E. Castellanos-Alvarez[2], D. Del Angel-López[1]

[1]*Instituto Politécnico Nacional, CICATA-Altamira, km. 14.5 Carretera Tampico-Puerto Industrial Altamira. C.P. 89600. Altamira, Tamps., México.*
[2]*Student of PMTA, CICATA-Altamira, Instituto Politécnico Nacional, Km. 14.5, Carretera Tampico-Puerto Industrial Altamira. C.P. 89600. Altamira, Tamps., México.*
[3]*Instituto Politécnico Nacional, CMP+L, Av. Acueducto s/n, Barrio La Laguna, Col. Ticomán, C.P. 07340, Ciudad de México, México.*

Received: January 17, 2018; Accepted: May 21, 2018

Abstract

High density polyethylene (HDPE)/polylactic acid (PLA) polymer blends were synthesized by the extrusion process using different molar ratios (95:5, 90:10, 85:15 and 80:20) in order to evaluate the effects on their structural, morphological and mechanical properties as well as on the degradation rate. The as-obtained materials were characterized structurally, chemically, thermally and morphologically by Fourier transform infrared spectroscopy (FTIR), X-ray diffraction (XRD), differential scanning calorimetry (DSC), atomic force microscopy (AFM) and scanning electron microscopy (SEM). The mechanical properties of the extruded blends were characterized by the tensile and impact test, whilst the degradation process was studied by environmental composting and accelerated weathering. Independently of the PLA amount, the samples showed coarse droplet morphology; however, it causes an important crystallinity reduction. Slight changes in the mechanical and thermal properties were also observed. The best performance was achieved with the 85/15 molar ratio, which showed a lifetime decrease close to 60% in comparison with HDPE.

Keywords: high density polyethylene; polylactic acid; polymeric blends; extrusion; degradation.

Resumen

Diferentes relaciones molares de mezclas poliméricas de polietileno de alta densidad (PEAD)/ácido poliláctico (APL), 95:5, 90:10, 85:15 and 80:20, se prepararon utilizando un proceso de extrusión con el fin de evaluar la influencia de la composición en las propiedades estructurales, morfológicas y mecánicas, así como su velocidad de degradación. Las muestras preparadas fueron por lo tanto caracterizadas estructural, química, térmica y morfológicamente utilizando las técnicas de espectroscopia por transformada de Fourier (FTIR), difracción de rayos-X (XRD) calorimetría de barrido diferencial (DSC), microscopia de fuerza atómica (AFM) y microscopia electrónica de barrido (SEM). Las propiedades mecánicas de las muestras extruidas se determinaron mediante pruebas de tracción e impacto mientras que, los estudios de degradación se realizaron mediante pruebas de compostaje ambiente e intemperismo acelerado. Independientemente de la cantidad de PLA, las muestras presentaron una morfología en forma de gota gruesa; sin embargo, al incrementar PLA se causa una disminución importante en la cristalinidad. Cambios muy pequeños se observaron en las propiedades térmicas y mecánicas. Un desempeño más relevante en función de las propiedades observadas se obtuvo con una relación 85/15, la cual presentó también una disminución en el tiempo de vida de hasta un 60% en comparación con HDPE puro.

Palabras clave: polietileno de alta densidad; ácido poliláctico; mezclas poliméricas; extrusión; degradación.

* *Corresponding author. E-mail*: atohuer@hotmail.com
doi: https://doi.org/10.24275/uam/izt/dcbi/revmexingquim/2019v18n1/Torres
issn-e: 2395-8472

1 Introduction

Many of the physical and chemical properties of plastics make them ideal materials for a wide variety of products and applications. However, because of their excellent mechanical properties, their increased use, mainly as packaging materials, has led to substantial environmental pollution. Although they are useful and desirable for many purposes, the indestructibility of petroleum - based plastics is a growing concern because of their accumulation in the environment (van Franeker and Law 2015). The plastics that are most widely used have poor degradability and may have lifetimes of hundreds of years when buried in typical solid-waste sites. This kind of polymers, due to their relatively new presence on the planet, are resistant to microbial attack since nature has not been able to design new enzyme structures capable of degrading them (Mueller 2006). One of the main plastics present in municipal solid waste matter is high density polyethylene (HDPE), a semi-crystalline thermoplastic with a linear CH_2-CH_2 chain structure with few branching, non-toxic, with acceptable chemical resistance and good mechanical strength, characteristics that make of it an attractive material for the production of plastic bags, toys, cases (elbow, knee), household items; it is also widely used in the automotive and food packaging industry. The widespread use of HDPE and its high persistence in the environment have led to seek for solutions to reduce the presence of this polymer in the environment (Martínez Romo *et al*. 2015).

An approach to reduce the HDPE pollution problem is by accelerating the polymer degradation process either through physical or chemical modifications caused by naturally occurring polymers. Blends of synthetic polymers with natural ones have become an economical and versatile route to obtain polymers with a wide range of desirable properties. Through this method, partially biodegradable polymers can be obtained and the volume of plastic waste effectively reduced via partial degradation (Garg and Jana 2007, Leja and Lewandowicz 2010). The amount of biodegradable polymer in the blend is a determinant factor to achieve the attack by microorganisms (Chandra and Rustgi 1998, Ali Shah *et al*. 2008). During the polymer degradation, physical or chemical changes occur as a result of diverse environmental factors such as light, heat, moisture, chemical conditions or biological activity resulting in bond scission and side-chain branching and subsequent chemical transformations and formation of new functional groups, which in turn provoke visual changes, for example, crazing, cracking, erosion, discoloration, phase separation or delamination (Pospisil and Nespurek 1997). Thus, after chain scission takes place, free radicals can react with oxygen or form secondary radicals by abstraction of a hydrogen atom leading to long chain branching and several oxidation products (Cuadri and Martín-Alfonso 2017). It is also highly desirable that these materials must present a high processability, mechanical properties and stability comparable to those characteristics featured by non-degradable polymers (Leon Janssen and Moscicki 2009).

PLA is a biodegradable polymer (i.e., polymers that are engineered to be biodegraded completely in a microbial environment) derived from starch and it is the main biopolymer that is commercialized as a biodegradable packaging material. PLA properties such as melting point, mechanical strength and crystallinity are determined by the polymer architecture and molecular mass. Although PLA is a growing alternative as a green food packaging material (Kale 2006), it has drawbacks such as low toughness, high production cost, brittleness, poor water vapor/gas barrier properties and undesirable thermal stability, which make this bioplastic unsuitable for certain applications (Arjmandi *et al*. 2015).

Most of the recent research works have been focused on the modification of existing products with PLA to generate new degradable alternatives via different mechanisms such as biodegradation, photo-degradation, environmental erosion and thermal degradation or a combination of them (Kawai 1995, Kang *et al*. 2015, Gorrasi *et al*.2013, Huang *et al*. 2015; b Madhu *et al*. 2014; Madhu *et al*. 2015). For example, blends of PLA and polystyrene (PS) have been prepared to balance the PLA cost and enhance the PS degradability. The properties of such blends are between those of pure PLA and pure PS, and have potential applications in medical devices and packaging products(Mishra *et al*. 2001, Hamad *et al*. 2011, Soroudi and Jakubowicz 2013, Scaffaro *et al*. 2011, Yuan and Favis 2004).La Mantia *et al*. (2012) demonstrated that small amounts of PLA in the PET waste can significantly affect the rheological properties under non-isothermal elongational flow. Our research group has also shown that the interaction between both polymers (PET/PLA) is trough secondary bonds by hydrogen bridges and electrostatic forces, good miscibility and an increase

in the PLA amount in the blends, increases the degradation of the materials (Torres-Huerta *et al*. 2014).

The crystallization, hydrolytic degradation and mechanical properties of poly(trimethylene terephthalate) and PLA blends have also been reported (Zou *et al*. 2009), whereas Kang *et al*. (2015) reported the effect of adding different proportions of PLA to a polypropylene (PP) matrix by melt-compounding on the miscibility, phase morphology, thermal behavior, and mechanical and rheological properties.

Commonly, PLA and polyethylene (PE) blends have been reported to determine the effect of polyethylene on polylactide degradation (a Madhu *et al*. 2014; Madhu *et al*. 2015; a Madhu *et al*. 2016; b Madhu *et al*. 2016) and based on thermodynamic data, it has been demonstrated that PLA and PE are very immiscible, therefore, sometimes, a block copolymer is required for assessing these blends (Raghavan and Emekalam 2001, Sinclair 1993, Sinclair and Preston 1993). A deep understanding of how the degradation rates of PE/PLA blends can be modified without affecting other important properties (mechanical) is still mandatory. It is worth underlining that in all the works mentioned above, PLA has been generally used to reduce the negative environmental impact of plastic waste, decrease the cost of the material and accelerate the degradation process (a Madhu *et al*. 2014; Madhu *et al*. 2015; a Madhu *et al*. 2016; b Madhu *et al*. 2016). Thus, the aim of this work is to accelerate the degradation of high density polyethylene (HDPE) by modifying its crystallinity while incorporating different amounts of PLA (5, 10, 15 and 20 wt-%) through single extrusion process without using compatibilizers agents.

Structural, morphological and mechanical properties are discussed in terms of the PLA content in the polymer matrix, HDPE. The novelty of this work is that focuses on investigation of the mechanical and structural properties of the HDPE/PLA blends subjected to natural outdoor in a region where the conditions are extreme in terms of humidity and temperatures, Altamira, Tamaulipas, México. This article provides a perspective of degradation and will complement the previous studies of degradation of HDPE/PLA. Additionally, the thermal and structural changes under accelerated weathering test were included to determinate the differences between natural conditions and oxidation degradation.

2 Materials and methods

The materials used in this study were high density polyethylene, HDPE (Alathon L5005), and polylactic acid, PLA (Ingeo 2002D), from Pochteca group distributor and PromaPlast resins, respectively. PLA is characterized by: its high molecular weight polymer with a number-average molecular weight (M_n) of 110,000 g/mol, weight-average molecular weight (M_w) of 914,000 g/mol, melting point temperature T_m= 210 °C, glass temperature T_g= 55-58 °C, density 1240 kg/m and melt flow rate of 5-7 g/10 min (210 °C/2.16 kg). HDPE has high molecular weight polymer with a number-average molecular weight (M_n) of 12,010 g/mol, weight-average molecular weight (M_w) of 299,484 g/mol, melt flow rate of 0.06 g/10 min (190 °C/2.16 kg), density of .949 g/cm^3, melting point temperature T_m= 199-216 °C.

Pellets were mixed thoroughly and then processed in a single screw extruder (Beutelspacher brand) (length to diameter ratio L/D = 30) to obtain blends with different HDPE/PLA weight ratios (95/5, 90/10, 85/15 and 80/20, wt-%).

Table 1. Temperature Profiles during extrusion process.

Blends (wt-%)	**Temperature (°C)**			**Screw speed (rpm)**	**MFI (g/10 min) 230 °C – 5 kg**
HDPE/PLA	**Zone 1**	**Zone 2**	**Zone 3**		
100/0	195	195	200	100	0.10 ± 0.01
95/5	193	193	195	80	0.11 ± 0.01
90/10	190	190	195	70	0.12 ± 0.01
85/15	185	185	190	66	0.13 ± 0.01
80/20	180	180	185	52	0.14 ± 0.01
0/100	-	-	-	-	114.17 ± 0.01

2.1 Characterization

Chemical characterization of polymer blends was carried out using a Perkin Elmer Spectrum One spectrometer (FT-IR) equipped with an attenuated total reflectance (ATR) accessory between 4000-600 cm^{-1} range at room temperature and an optical resolution of 2 cm^{-1} (20 scans). The sample characterization was performed before and after the composting process to evaluate the changes of the bands corresponding to the functional groups. It is important to mention that after six months in the compost environment, the samples were washed and dried for the FTIR analysis.

Structural characterization of the as-obtained blends was carried out using a Bruker D8 Advance diffractometer at room temperature, operating at 35 kV and 25 mA with CuKα radiation in the θ-2θ range of 10-60° and a scan speed of 1.5° min^{-1}.

Differential Scanning Calorimetry (DSC) measurements were carried out on a Perkin-Elmer DSC Pyris 1. Samples with weights ranging from 5 to 8 mg were introduced into aluminum pans, undergoing heating and cooling processes. Firstly, the samples were maintained at 40 °C for 2 min before heating. The temperature was increased to 200 °C with a heating rate of 10 °C min^{-1} and it was held for 30 s (first heating scan) before cooling. Then, it was cooled to 40 °C at the same rate (second scan). From XRD and taking into account that the total area under the diffraction pattern is divided into one crystalline zone (I_c) and another amorphous zone (I_a), an estimation of the crystallinity degree was carried out by using the following formula (Chen *et al*. 2014):

$$\chi = \frac{I_c}{I_c + I_a} * 100 \quad (1)$$

The melt flow index (MFI) experiment was performed on a Tinius Olsen (MP 600 Melt Indexer) plastometer. The MFI was measured at 230 °C by applying pressure with a load of 5 kg. To study the mechanical properties of HDPE/PLA blends, a tensile test was conducted on the specimens by using a universal machine (Instron 4411) and probes were prepared by extrusion and injection methods according to the ASTM D 638 standard. 8 samples were deformed under tensile loading using a 5 kN load cell.

The impact Izod test was performed on the notched specimens as recommended by the ASTM D 256 standard and probes were prepared by extrusion and injection moulding, but due to the viscosity of the HDPE/PLA 80/20 blend, only injection moulding was used. 8 specimens were tested in accordance with the same standard. Before performing the tensile and impact tests, the specimens were maintained at 23 °C and 50% of humidity for 24 hours. Morphology of the as-prepared samples and samples after the fracture tensile and impact tests was observed by scanning electron microscopy (SEM, JSM JEOL 6300) at an acceleration voltage of 10 keV and a working distance of 15 mm. All the samples were coated with an Au-Pd thin film.

The topographic features of the blends were obtained with a Nanosurf Easy Scan 2TM microscope. During the atomic force microscopy (AFM) analysis, the non-contact mode was employed by using 20 nN of force and scanning areas of 50 μm x 50 μm at different points of the specimens.

Composting was prepared by mixing commercial compost and horse slurry in a 50:50 ratio (wt-%). The mixture was poured into 5 containers of 3 L in capacity and specimens of 7 cm x 2 cm and a thickness of 3 mm were buried in the containers. Samples were evaluated in triplicate for a period of six months in Altamira, Tamaulipas, México (November 2011-May 2012). The humidity (%), temperature and pH were monitored constantly. Samples were exposed to UV light under accelerated conditions at 60 °C for 8 h followed by 4 h of water condensation at 50 °C for 900 h of exposure in a QUV accelerated weathering chamber model QUV/Se (May 2012), using UV-B lamps (313 nm and 0.63 W/m^2) as radiation source.

3 Results and discussion

3.1 Chemical characterization by FTIR

FTIR is a very useful tool to distinguish the intermolecular interactions between the individual components in a polymer blend. Physical or chemical compatibility determine the final properties and from these, the mechanism and degradation rate can be estimated.

Figure 1 shows the FTIR spectra of the HDPE/PLA blends obtained by the extrusion process with the different wt-% ratios (95/5, 90/10, 85/15, and 80/20), and the spectra of their individuals components, HDPE and PLA, are also included.

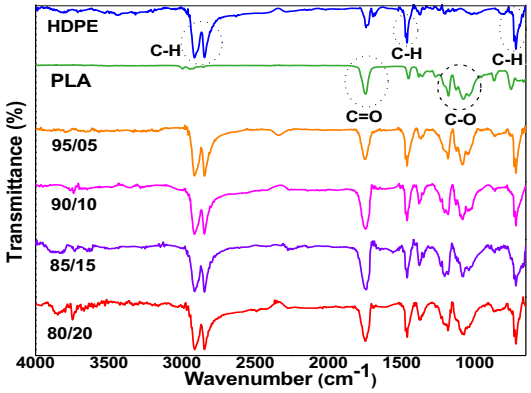

Fig. 1. FTIR of HDPE, PLA and HDPE/PLA blends obtained by extrusion process.

HDPE spectra show the signals corresponding to the asymmetric and symmetric vibrations of $-CH_2-$ at 2750 and 3000 cm^{-1}, respectively, where a small band located at 1750 cm^{-1} corresponds to the vibration of the carbonyl group $-C=O-$, which apparently appears as a consequence of the macromolecular breakdown caused by the thermo-oxidative degradation of HDPE, which took place at the outlet of the die (Musil and Zatloukal, 2011). The vibration of $-CH-$ deformation and the $-C-H-$ bending plane output band are found at 1490 and 720 cm^{-1}, respectively (Parthasarathi *et al.* 2010). In the spectra of pure PLA, the band located at 1750 cm^{-1} corresponds to the stretching of the ester carbonyl group $-C=O$, and the deformation of symmetric and asymmetric vibrations of $-CH-$ appears between the 1360-1460 cm^{-1} interval. Finally, the signals located at the 1050-1250 cm^{-1} interval correspond to the vibrations of the $-C-O$ and $-C-O-C$ stretching.

FTIR spectra of HDPE/PLA polymer blends confirm that the vibrational bands are the sum of the individual components of the blends. As expected, no appreciable shifts in the band of C−O bands in PLA or any other functional group were observed, ratifying the lack of chemical interaction or compatibility between the HDPE and PLA.

3.2 Structural studies by XRD

Figure 2 compares the XRD diffraction patterns of the raw materials and the as-prepared HDPE/PLA blends. The HDPE pattern shows the strong characteristic reflections of the orthorhombic structure assigned to the (110) and (200) planes at 21.8 and 24.2°.

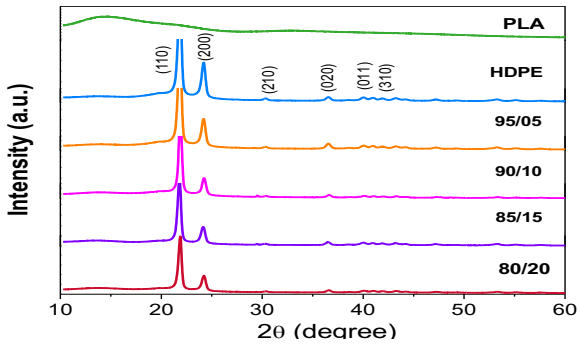

Fig. 2. X-ray diffraction patterns of HDPE, PLA and HDPE/PLA blends.

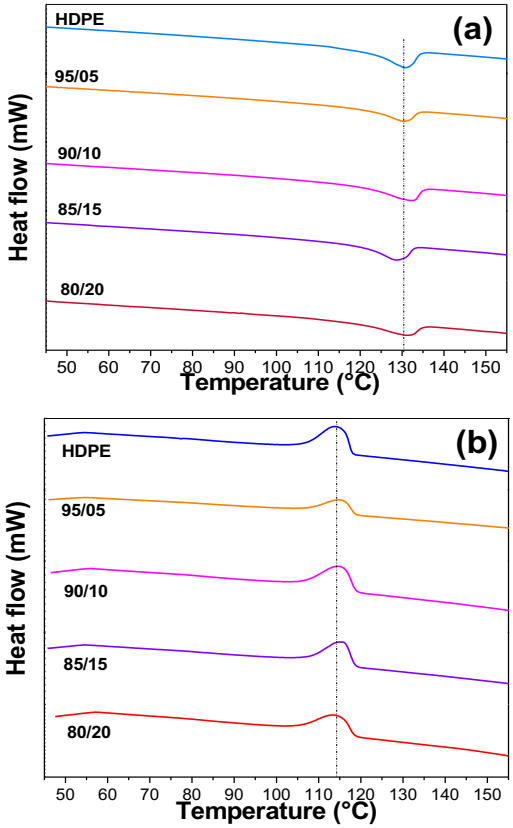

Fig. 3. DSC thermograms of HDPE/PLA blends: (a) melting temperature (T_m) and (b) crystallization temperature (Tc).

Other signals are identified according to ICDD Nr. 53-1859 corresponding to (210), (020), (011), (310), (111), (220) and (311) planes (Chouit *et al.* 2014), whereas PLA shows the typical peak of an semicrystalline polymeric matrix centered at 2θ degrees ca. 15°.

As it was expected, XRD patterns of the blends display only the corresponding reflections of HDPE; however, as the PLA content increases, the intensity of the peaks decreases.

3.3 Differential Scanning Calorimetry (DSC)

Figure 3a-b shows DSC thermograms of the pure HDPE and polymer blends with different quantities of PLA. A displacement of the crystallization temperature (Tc) towards higher temperature (115 °C) was observed in the polymer blends in comparison with pure HDPE. Besides in all polymers blends, the melting temperature (T_m) is augmented from 130 to 132 °C. It is well known that the Tc of PLA is ca. 126 °C with a T_m of 161 °C whereas for HDPE the Tc value is in the range of 110-120 °C with a T_m peak between 130-135 °C, thus the fact that only Tc and T_m appears in DSC thermograms indicate a strong physical interaction between the HDPE and PLA.

3.4 Determination of polymer crystallinity % by XRD data

XRD observations suggest that the PLA quantity reduces the crystallization process of HDPE and/or the crystallite size. Figure 4 shows an important reduction in the crystallinity percentage even with low PLA contents, and it reached a value of about 37% with an 80/20 ratio.

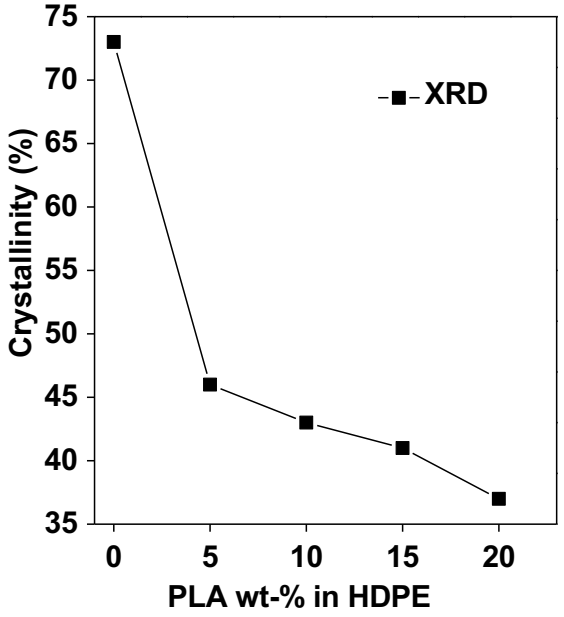

Fig. 4. Crystallinity % in HDPE/PLA blends.

Then, the PLA addition affects some of the main pathways during the HDPE crystallization: i) the formation of a critical nucleus on the front of the growing spherulite, ii) the diffusion in the chain through the matrix of other chains near the growing spherulite, and iii) the diffusion of the center of mass of the crystallizable polymer chains in HDPE towards the growing front (Oudhuis *et al*. 1994). PLA particles also seem to affect the mobility of HDPE chains, which prevents the chain rearrangement from happening easily during the crystallization process. Thus, the crystallization change of HDPE/PLA blends was determined mainly by the nucleation effect of PLA crystals and the effect of partial miscibility between these polymers.

HDPE/PLA blends processability was analyzed by measuring the melt flow index (MFI) at 230 °C in a Tinius Olsen MP600 Melt Plastometer (Zhang *et al*. 2015) and the results are also shown in Table 1. In agreement with previous reports using the ASTM D1238 standard (2004), the MFI of PLA (114.17 g/10 min) was much higher than that of pure HDPE (0.10 g/10 min). HDPE/PLA blends present a melt index value close to the value of HDPE neat polymers (Krässig *et al*. 1984, Harris and Starita, 2011). The inclusion of PLA in the HDPE polymer increases the mobility of macromolecular chains at the molten state, the material loses viscosity and therefore the processing speed is reduced with the biopolymer addition.

3.5 Morphological and topographical studies

Figure 5 shows typical SEM micrographs of HDPE/PLA polymer blends with different PLA amounts. The effect of different PLA quantities can be clearly seen in this Figure. The heterogeneity of the blends is obvious in all the cases, but significant differences can also be observed. Except with 5 wt-% of PLA, it is difficult to identify a continuous phase in both components, but the PLA immiscibility in the polymer matrix caused the discontinuity of the HDPE phase, which is seen in a globular morphology, with spherical droplets of the PLA phase suspended in the HDPE. PLA is uniformly dispersed with 5 wt-% of PLA and began to agglomerate after 10 wt-%. This is attributed to the combination of low interfacial adhesion between the HDPE and PLA phases, and to a much lower viscosity of the PLA phase dispersed in the HDPE matrix with higher viscosity.

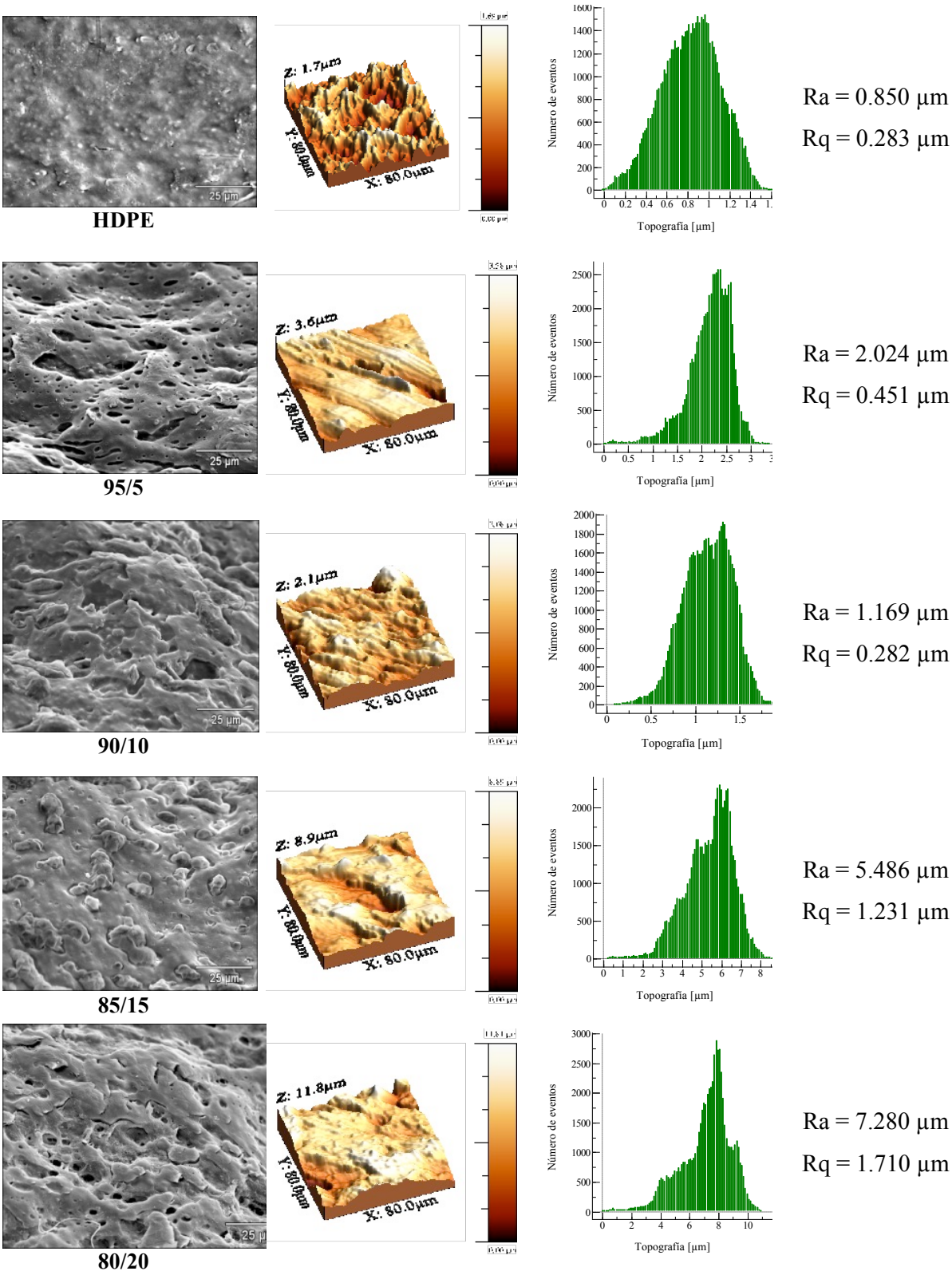

Fig. 5. SEM and AFM images of as-prepared HDPE/PLA blends.

The ratio of the theoretical viscosities is lower than 1 (η_{PLA}/η_{HDPE}=0.01) allowing a coarse droplet morphology. The viscosity ratio plays a major role in the morphology evolution (a less viscous phase encapsulates a more viscous phase) (Magonov *et al*. 1997). Irregularly distributed barrier layers or droplets can increase the degradation rate of the blends but at the same time reduce the processability of the blends.

The heterogeneous structure was also observed by atomic force microscopy (AFM) measurements. AFM is extremely useful for the study of polymer surfaces because it provides real-space polymer surface profiles and nanostructures (Monticelli *et al*. 2014). The tests have been performed on ternary samples polymer blends based on Polylactide/high-density polyethylene/poly(styrene-ethylene/butylene-styrene) triblock copolymer (PLA/HDPE/SEBS) (Jun Wang *et al*.). Height and phase imaging contact mode across the length scales were used to investigate the topography and roughness dependence on the PLA content (Figure 5).

In this figure, R_a is the average surface roughness; R_q is the quadratic surface roughness that is the mean square of the Z data and the roughness distribution graph (topography in μm vs number of events) in the evaluated area of 80 μm^2. The surface roughness is one of the quantitative magnitudes that describes the surface relief. In this case, the Z value is defined as the difference between the highest and lowest points within the given area. The color code in this figure corresponds to variations in the phase signal, which shows clearly the topography and domains indicative of the two blend components. The oriented topography of the HDPE/PLA blends may result from the processing. The R_a and R_q values were increased from 0.850 (0.283) μm for the HDPE pure sample to 2.024 (0.451), 1.169 (0.282), 5.486 (1.231) and 7.280 (1.710) μm for the HDPE/PLA samples with 95/5, 90/10, 85/15 and 80/20 weight ratios, respectively. The trend in the obtained values supports the SEM observations, where holes and agglomerates increase in size with the increasing amount of biopolymer in the HDPE matrix. One of the main reasons for the lack of compatibilization is due to the absent of a compatibilizer that would produce synergistic effects between HDPE and PLA (Dikobe *et al*. 2017). Due to this, it would be necessary to include compatibilizers or coupling agents to prevent the heterogeneity and improve the bonding between phases.

3.6 Mechanical properties

The composition dependence of some properties may give information about structure and interaction changes. However, not all properties respond to these factors equally sensitively and similarly; for example, properties measured at large deformations show the modification of the interfacial adhesion much better than the modulus. Table 2 displays the recorded value dependence of the tensile strength (MPa) and break elongation (%) of blends as a function of PLA content and a comparison with pure HDPE. PLA is well known as a glassy polymer at room temperature, which displays maximum strength (65 MPa) with low break deformation (9%) (Monticelli *et al*. 2014). In comparison to PLA, HDPE has the lowest resistance (22.30 MPa) which is similar to the value reported (24.40 MPa) by Sinclair, but it shows higher break elongation (988%) (Sinclair 1993). The tensile strength of the HDPE/PLA blends decreased gradually with the amount added of PLA, but a drastic diminution was observed when 20 wt-% of PLA was added to the neat HDPE matrix. The addition of a high content of PLA decreased the tensile strength from 22 to 14.60 MPa, indicating that the final blend was more brittle than it had been expected (Petinakis *et al*. 2013).

Table 2. Dataset of tensile strength, elongation at break of HDPE and its blends with PLA.

HDPE/PLA	**Tensile strength (MPa)**	**Elongation at break** (%)	**Izod impact energy (J m^{-1})**	**Interparticulate distance ID (μm)**
100/0	22.0 ± 0.60	988	111± 11	
95/5	20.3± 3.47	988.1	94 ± 6	0.276
90/10	19.2± 1.12	987.9	81 ± 15	0.176
85/15	19.7 ± 4.21	917.5	42 ± 2	0.127
80/20	14.6 ± 12.98	235.7	64 ±7	0.096

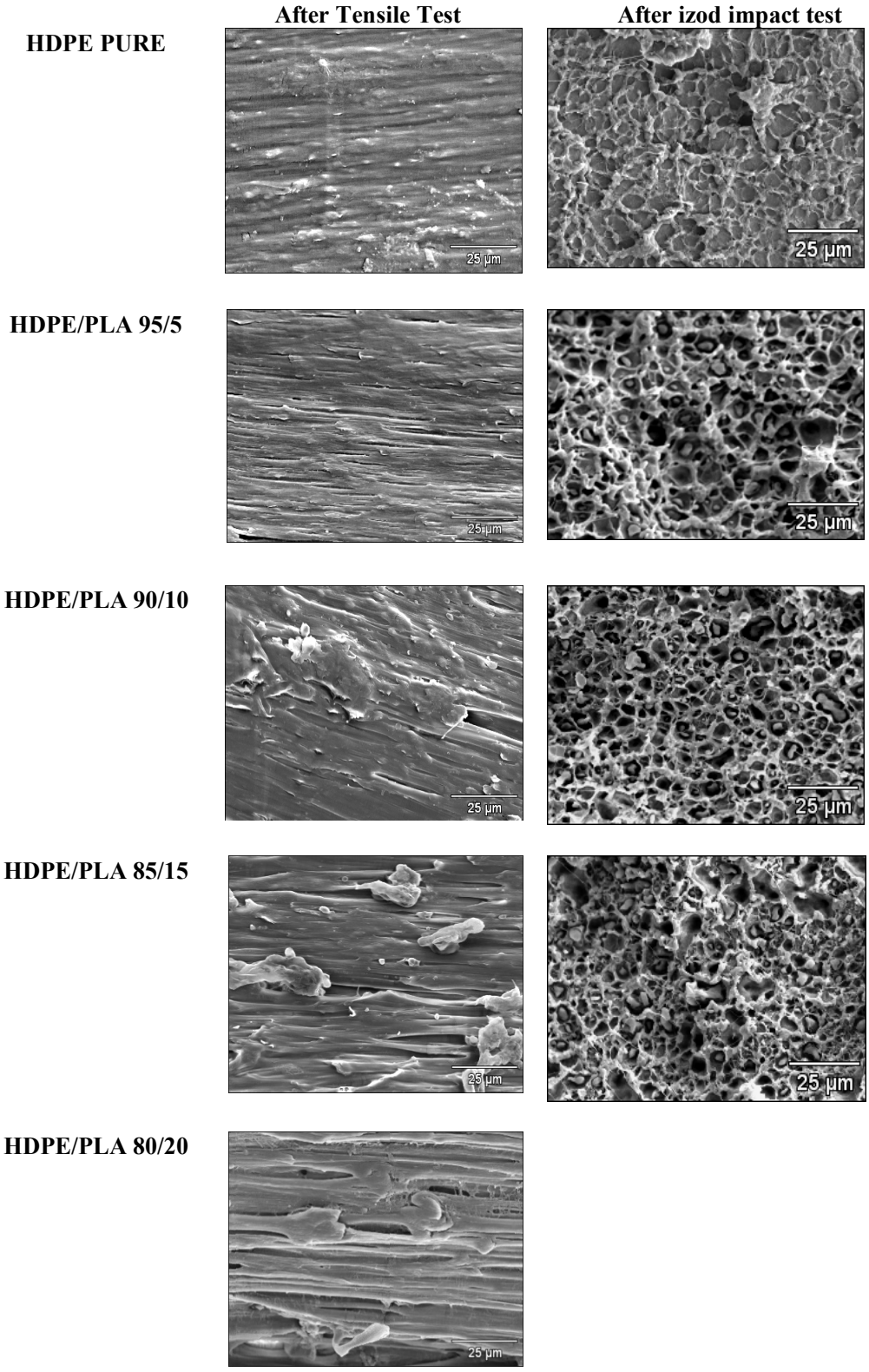

Fig. 6. SEM images of fractured samples after tensile and izod impact test.

An adequate agreement was observed in the elongation properties with the break point of the as-prepared polymer blends, where samples with 20% of PLA showed an important reduction in the elongation with values ca. 76% in comparison with pure HDPE (988%). The trend of the results is in good agreement with previous reports using other kinds of thermoplastics and similar studies of HDPE/PLA blends (Sinclair 1993, Ploypetchara *et al*. 2014). A possible explanation of this behavior is again related to the weak physical interaction between PLA and HDPE, provoking large agglomerates, which act as a stress concentrator, provoking the sample failure during the tensile process. Another possibility is related to the formation of a dense material structure, which prevents the plastic from flowing along the tensile direction. Table 2 also shows the notched Izod impact energies of neat HDPE and HDPE/PLA blends containing different PLA ratios. HDPE/PLA ratios of 95/5 and 90/10 displayed a reduction to 94 and 81 J m^{-1} of impact strength with respect to the neat HDPE matrix (111 J m^{-1}). This decline in the properties is associated with the crystallinity modification of the blends by the addition of an amorphous minor phase (Nerkar *et al*. 2015). This trend is also observed with the addition of 15 wt-% of PLA, where the Izod impact energy decreased up to 42 J m^{-1}; however, an opposite effect occurred with 20 wt-% of PLA (64 J m^{-1}). This behavior may be related with the preparation method, i.e. HDPE/PLA (80/20) samples were obtained by high pressure-injection method, in comparison with the counterparts where we used low pressure injection.

It is well known that the impact strength is the sum of the contributions of all processes that dissipate the impact energy, including the morphological and structural characteristics of the blends. Thus, the impact strength is modified positively either by decreasing the particle size or by increasing the dispersed phase concentration (i.e. the number of dispersed particles) since the brittle-ductile transition occurs at a critical value of the interparticulate distance (ID) (Lee and Chun 1998, Loyens and Groeninckx 2002). To study the ID effect on the brittle-ductile transition (BDT), an approximation was used, which was the ID equation of an elastomer-filled system (Yuan *et al*. 2001):

$$ID = D\left[\left(\frac{\pi}{6\phi_r}\right)^{1/3} - 1\right] \qquad (2)$$

where D is the dispersed phase particle diameter (PLA), ID is the interparticle distance and ϕ_r is the volume concentration (PLA). ϕ_r can be calculated with the PLA weight fraction, PLA density and the HDPE matrix density:

$$\phi_r = \frac{W_{PLA} \cdot \rho_{PLA}}{W_{PLA} \cdot \rho_{PLA} + (1 - W_{PLA})\rho_{HDPE}} \qquad (3)$$

ID varied from 0.276 to 0.096 μm (Table 2). The results indicate that the transition from notch brittle behavior to notch tough behavior can be achieved with the decreased ID by increasing the proportion of PLA (i.e. 20 wt-%); however, it should be kept in mind that high impact strength does not necessarily imply ductile failure and brittle fracture does not necessarily imply low impact strength even though it fractures in a brittle manner. SEM micrographs were used to evaluate the morphology of the tensile-failed surface and Izod impact fractured samples to determine the characteristic surface patterns that generally accompany a specific polymer. It is worth noting that HDPE is a ductile polymer with apparent yielding and cold-drawing behavior, whereas PLA is a brittle polymer without yielding during the universal tensile process. To analyze the behavior of combining both polymers, Figure 6 shows the SEM micrographs of the stretched tensile specimens. A comparison of the SEM images of pure HDPE versus the different HDPE/PLA blends showed that PLA induced a definite decrease in elongation to fracture, which became more substantial for some samples (85/15, 80/20). Elongated cavities are clearly visible around the de-bonded PLA particles. The final fracture of the samples is probably initiated by large agglomerates or large particle sizes of PLA in the specimen located by the propagating neck. This fact suggested extensive de-bonding of the PLA particles from the matrix occurring near the yield point and confirmed a state of low adhesion between components (Wilbrink *et al*. 2001).

Figure 6 also shows the SEM micrographs of notched fractured surfaces of the pure HDPE and HDPE/PLA blends with ratios of 95/5, 91/10 and 85/15, respectively. All the samples exhibited brittle fracture without plastic deformation observable on the fracture surface. It can be observed that by increasing the PLA amount in the HDPE polymer matrix there is a proportional increase in the quantity of small holes in the fracture surface, probably due to the fact that PLA makes HDPE more brittle and increases the degradability process.

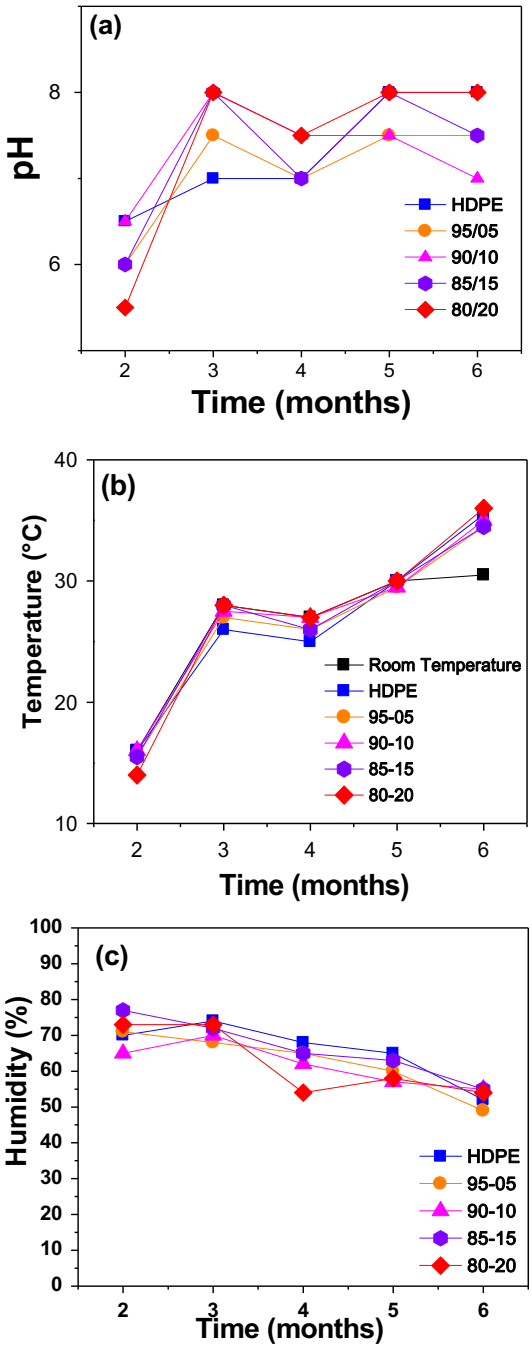

Fig. 7. Data variation of composting conditions, (a) pH, (b) temperature and (c) humidity.

By performing a comprehensive analysis of all the micrographs presented in Figure 6, it can be said that the PLA amount exerts an important effect on the mechanical properties since these dots become yield point and could affect proportionally the degradation process of HDPE.

3.7 Composting degradation

Microorganism such as bacteria and fungi are involved in the degradation of both natural and synthetic plastics (Gu *et al*. 2011). The biodegradation of plastics proceeds actively under different soil conditions according to their properties because the microorganisms responsible for the degradation differ from each other and they have their own optimal growth conditions in the soil. Biodegradation is governed by different factors that include polymer characteristics such as mobility, tacticity, crystallinity, molecular weight, the type of functional groups and substituents present in the structure (Artham and Doble 2008). In this work, the composting studies were carried out in pure HDPE (as standard) and HDPE/PLA polymer blends to establish the degradation process and propose a mechanism. During the degradation process, variables such as pH, temperature and humidity were monitored (see Figure 7 a-c) as follows: pH range of 5-8, temperatures between 15 to 38 °C and humidity of 45-80%. These factors are consistent with those reported in the literature (Meneses *et al*. 2007). Test specimens of pure HDPE and HDPE/PLA blends were exposed to biodegradation for 6 months in a mixture of commercial compost with horse slurry (50:50 wt-%). Three test specimens were tested for each composition.

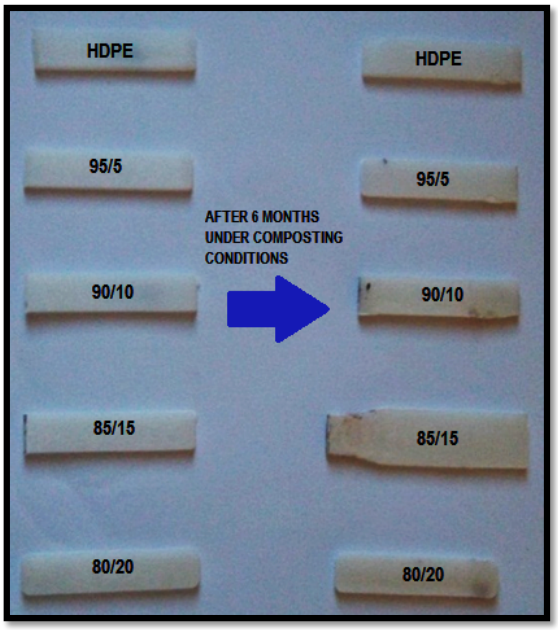

Fig. 8. Images of samples before and after composting degradation.

The visual aspects of these biodegraded samples are presented in Figure 8 (Samples on the left were not buried, they were selected to show the change in visual aspects after degradation), where the HDPE/PLA blends shows more evident alterations in color than the pure HDPE. The HDPE/PLA blends show a yellowing effect that occurs due to the fact that the PLA chains begin to degrade it. This color change is more noticeable in blends with a higher content of biopolymer, indicating an increasing susceptibility to degradation and it is expected that the material will degrade faster than those materials with lower biopolymer blend contents.

To evaluate the biodegradation extent of the HDPE polymer and blends, FTIR spectra of non-biodegraded and biodegraded samples were compared (Figure 9). FTIR spectra of HDPE/PLA blends (5-15 wt-%) showed a significant reduction in all the bands related to PLA, while the ones associated with HDPE, mainly the band related to CH_2 groups are still present. The C=O band correlated with the oxidative degradation during the extrusion process is missing in the FTIR spectra evaluated after the composting test, which confirms that the HDPE degradation process starts with C=O groups, which are more susceptible to degradation than the C−H groups. The reduction of bands related to C=O (~1750 cm^{-1}) and C−O (~1100 cm^{-1}) is attributable to scission of PLA chains, which in turn is higher with the PLA amount present in the HDPE/PLA blends. In summary, samples with PLA amounts between 5-15 wt-% showed a significant reduction in the intensity of C=O and C−O, peaks that can be broken by the hydrolytic degradation of the ester bonds and the shortening of the aliphatic chains.

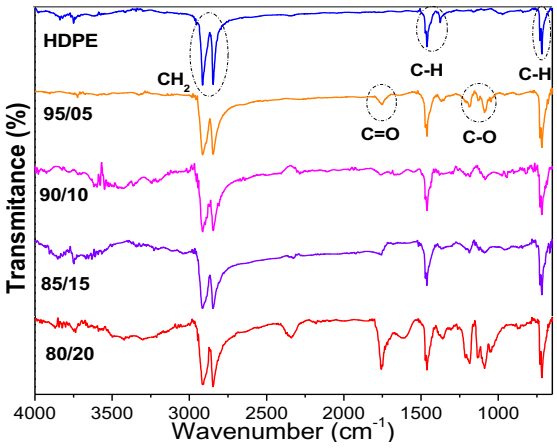

Fig. 9. FTIR spectra of HDPE/PLA blends after composting degradation.

During an aerobic biodegradation, the microorganisms use oxygen and consume carbon from the polymer as a food source; as a result, carbon dioxide and water are produced and released since this reduction might have been due to the metabolism of oxygen consumption by the microorganisms (Moura *et al*. 2011). The HDPE/PLA (80/20) blend did not show any diminution of C=O and C−O signals; however, it is well known that during a strong degradation process, a widening or shifting in the carbonyl signal due to the overlapping of ester carbonyl and carboxylic acid bands is produced (1750 and 1725 cm^{-1}). Another important observation is the appearance of a new band at 1612 cm^{-1} that is attributed to the formation of carboxylate chain end groups during the hydrolysis (Wang *et al*. 2013). Hence, an increase in PLA amount contributes to accelerate the HDPE degradation process. The hydrolytic degradation of PLA gives rise to the O−H groups that are missing in the FTIR analysis due to the drying process that was performed before the analysis as described in the experimental section.

It is also recognized that the biodegradation process under aerobic conditions can be described with the following reaction (Rundnik and Briassoulis 2011):

$$C_{polymer} + O_2 \longrightarrow CO_2H_2O + C_{scraps} + C_{biomassa} + salts$$

3.8 *Mechanical and thermal properties after degradation tests*

In order to verify changes in the mechanical properties of the biodegraded specimens, impact resistance results are shown in Figure 10. The pure HDPE sample, after 6 months of composting degradation, showed a significant increase in the impact strength from 123 to 705 J/m, which seems to corroborate that in the first degradation stage, the amorphous regions are degraded, and subsequently, the crystalline regions become amorphous, continuing the degradation process. During the evaluation time of this study (six months), only the first changes were observed, which were produced as a consequence of the compost degradation, when the amorphous phase of the polymer or polymer blend is almost completely degraded (Sudhakar *et al*. 2008). During the evaluation time, the crystallinity of HDPE was increased, which may explain the impact strength values, i.e. samples subjected to the composting test displayed the well-known microorganism attack, which eats the amorphous phase of HDPE, causing higher crystallinity in the samples.

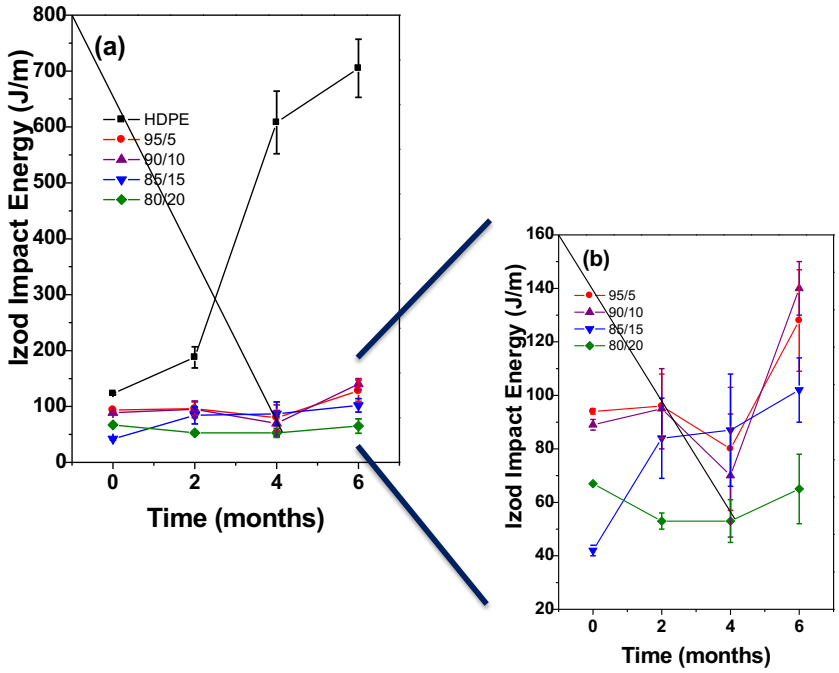

Fig. 10. Images of samples before and after accelerated weathering test.

It is important to mention that it is expected that longer periods of time in the composting process will present the opposite effect and brittleness in the plastic material. In the HDPE/PLA blends, the impact resistance after composting degradation is much lower than that of pure HDPE with values in the 40-140 J m^{-1} range. Specifically with 5 and 10 wt-% of PLA, the behavior is almost the same; in the first two months, the impact strength is maintained at around 94 J m^{-1}; in the fourth month, this value decreased to 80 and 70 J m^{-1}, respectively; finally, in the six month, this resistance was increased again to 128 and 139 J m^{-1}.

By comparing the as-prepared samples containing 15 wt-% with those having 5 and 10 wt-% of PLA, an expected increase in the impact strength from 41 to 101 J m^{-1} was observed, which was due to the PLA brittle nature. A similar trend is observed in the sample with 20 wt-%, presenting values of 67±1, 53±3, 52±8 and 65±13 J m^{-1}; the increase in the standard deviation after the fourth month of composting degradation is correlated with the increasing inhomogeneity of the samples due to PLA degradation, which caused imperfections in the sample surfaces. The PLA content reduced the Izod impact energy, but at the same time, it can provoke strong agglomerations that affect the overall mechanical properties. It is also clear that in the samples, the microorganism consume, in the first stage, the biodegradable polymer phase (PLA) followed by the amorphous phase, and finally by the crystalline HDPE phase. A compost environment controlling the parameters of pH, humidity and temperature provokes a biotic chemical degradation where the microbial species are adhered to the surface of the HDPE and HDPE/PLA blend samples; it has been reported that this adhesion is due to a kind of substance of complex matrix made of polymers (polysaccharides and proteins) (Vu *et al*. 2009); this substance infiltrates the porous structures of the polymers and alters their size and distribution, changes the moisture degrees and the thermal transfer within the material. The function of this substance (slime matter) is to protect the microorganisms against unfavorable conditions (desiccation and UV radiation). The mechanical action of the microorganisms is to increase the size of pores and provoke cracks. Thus, the resistance and durability of the material is physically weakened (Lucas *et al*. 2008).

Once this physical interaction takes place, the extracellular polymers, produced by the microorganisms, act as surfactants that facilitate the exchanges between the hydrophilic and hydrophobic phases. These interactions favor the penetration of

microbial species and, as a consequence, contribute to the chemical biodeterioration; water also penetrates the polymer matrix and initiates the hydrolysis of PLA at the ester carbonyl bonds; PLA features low degradability under neutral conditions and higher degradability under basic conditions as in this case. Most polymers are too large to pass through cellular membranes, so they must first be depolymerized to smaller molecules before they can be absorbed and biodegraded within microbial cells (Ali Shah *et al*. 2008). From the overall results, HDPE/PLA (85/15) provided a balance between the mechanical properties and degradation time, which suggested a potential use in industrial applications.

3.9 Accelerated weathering

Figure 11 reveals the physical changes in the blends and neat HDPE after 900 h of exposure to the accelerated weathering chamber; the obtained results show that after 900 hours of exposure, the material shows a significant color change (yellow) and this color is more evident in biopolymer blends whose proportions are higher (85/15 and 80/20). To analyze the chemical bonds of these samples, FT-IR studies were performed and the results are shown in Figure 12. The FTIR spectra show bands at 2927-2845 cm^{-1} which are correlated to the asymmetric and symmetric vibrations of $-CH_2-$ groups. Bands located at 1200 and 1000 cm^{-1} are attributed to ester (–CO–), and the band at 1750 cm^{-1} corresponds to the stretching of carboxylic acid. The reduction in the intensity of the bands and slight shifting to lower wavelength ranges (1200-1000 cm^{-1}) proved that the degradation mechanism occurred predominantly by ester bond hydrolysis.

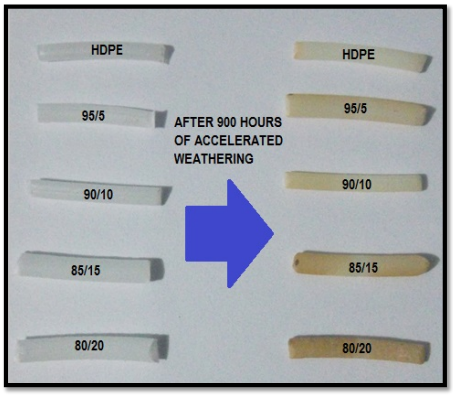

Fig. 11. FTIR spectroscopy for HDPE and HDPE/PLA blends after 900 h of exposure to accelerated weathering chamber.

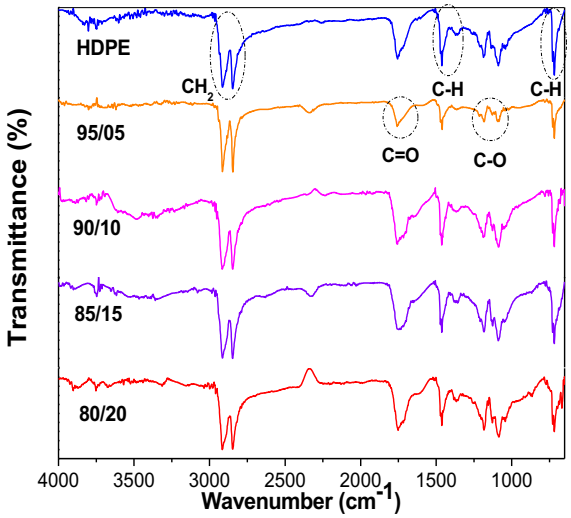

Fig. 12. Weight loss (%) of pure HDPE and HDPE/PLA blends after exposure to the accelerated weathering chamber for 900 h.

In order to compare both methods, broader bands in the 1750-1000 cm^{-1} range are observed after accelerating weathering process, whereas composting degradation highlights that except for an 80/20 weight ratio, the bands are correlated with ester (–CO–), and carboxylic acid bonds tend to disappear.

The degradation mechanism mismatch can be due to the fact that during the weathering tests, the polymer chains break, provoking an increase in the quantity of carbonyl groups, facilitating the polymer degradation (Stark and Matuana 2004). Different researchers have proposed that carbonyl groups are the main UV light absorbing species responsible for the photo-initiation reactions in polyethylene (Jabarin and Lofgren 1994, Wypych 2013, Kaci *et al*. 2000, Muasher *et al*. 2006).

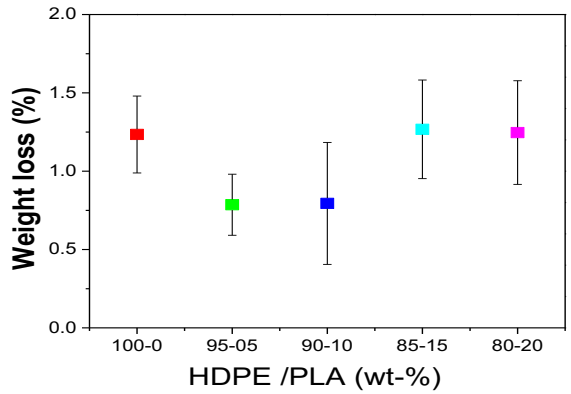

Fig. 13. DSC thermograms of HDPE/PLA blends after accelerated weathering.

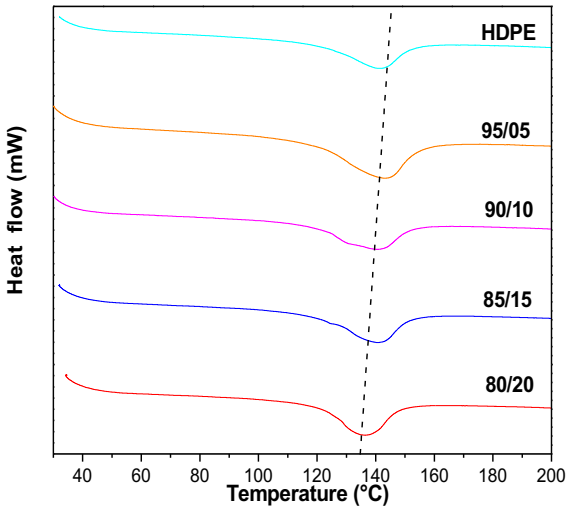

Fig. 14. Degradation rate of HDPE/PLA blends.

Moreover, the reduction of the carbonyl bands during the composting degradation can be due to the metabolism of oxygen-consuming microorganisms. Figure 13 shows weight loss percentages of each HDPE/PLA polymer blend and neat HDPE after 900 h of exposure to the chamber. The weight loss varied from 0.78 to 1.25% depending on the amount of PLA in the biopolymer blends. In this sense, well-known steps during the biodegradation of polyesters are: i) polymer embrittlement, and ii) the diffusion of low molecular weight oligomers out of the bulk polymer undoubtedly help to start the degradation process.

To evaluate the weight loss effect on the thermal properties, DSC studies were performed (Figure 14). The melting temperature of HDPE and HDPE/PLA blends was found to decrease with the PLA amount at different extents after 960 h of weathering, which could be attributed to the weight loss, which in turn increased number of chemical irregularities present in the HDPE molecule (Temiz *et al*. 2007, Peng *et al*., 2015). The lowering of the melting temperature results from the increase in crystal defects occurring with oxidative degradation of structures such as double bonds, oxygenated groups, chain ends and branch sites, which results in smaller crystals with more imperfections.

3.10 Degradation rate

In previous studies of PET/PLA blends, a relationship of 1000 h of accelerated weathering equaling to a year of natural weathering could be used as conservative data (Torres-Huerta *et al*. 2014), whereas other researchers have considered an estimation of approximately 25,000 h of exposure under accelerated aging tests of HDPE geomembranes comparable to 25 years of exposure (Islam *et al*. 2011). A lifespan close to 150 years at 25 °C has been established for the HDPE geomembrane in landfill applications (Kerry-Rowe and Sangam, 2002). Following the approach described in previous work (Torres-Huerta *et al*. 2014), the weight loss % (Eq. 5) was used to estimate the degradation rate of the formulations as well as HDPE (Eq. 6).

$$Weight\ loss\ \% = \frac{W_i - W_r}{W_i} \tag{4}$$

where W_i and W_r represent the initial and residual weights of the specimens, respectively.

$$Degradation\ rate = \frac{KW}{ATD} \tag{5}$$

Where K is a constant of conversion units to mm/year ($K = 8.76x10^4$), W is the weight loss (g), A is the area exposed (cm^2), T is the time (h) and D is the density of the material (g cm^{-3}). In general, as expected, the degradation rates of HDPE/PLA blends were enhanced with the quantity of PLA in comparison with pure HDPE (Figure 15). A special result must be highlighted when 20 wt-% of PLA is added to the HDPE polymer matrix. In this case, an unexpected diminishing in the degradation rate, in comparison with its predecessor, occurred; even this tendency was observed during the Izod strength measurements. This anomalous behavior is correlated with the low homogeneity of the polymer blend. It is obvious that the degradation of HDPE can be accelerated with the physical dispersion of PLA to obtain good miscibility by selecting a suitable technique, which in this case was a single extrusion process.

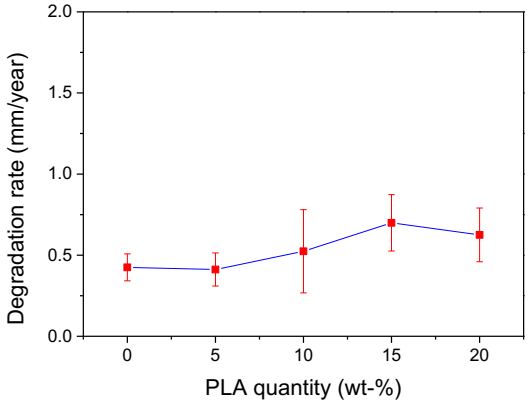

Fig. 15. Degradation mechanism proposed in composting degradation test.

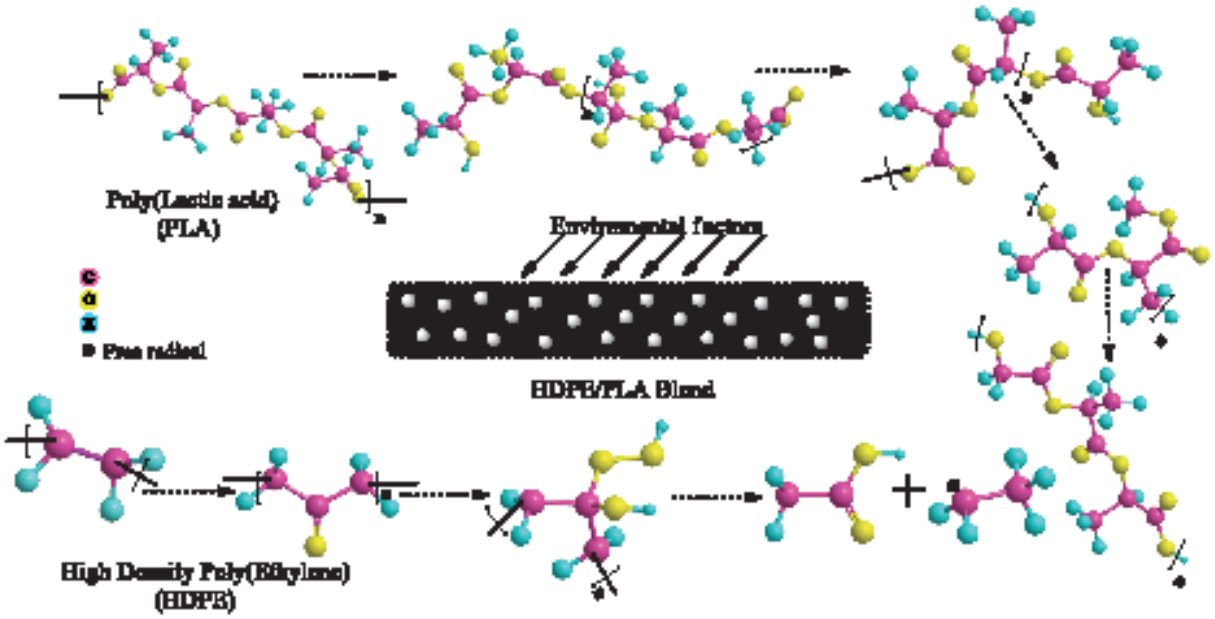

Fig. 16. Izod impact strength during the composting degradation test (a) full range graph (b) magnification from 20 to 160 J-m^{-1} range.

3.11 Degradation mechanism

Figure 16 shows a proposed mechanism for the composting degradation of HDPE/PLA blends; the results discussed above suggest that the degradation mechanism occurs through selective hydrolysis, where firstly, PLA begins to degrade and subsequently HDPE is degraded. PLA contains ester groups that have hydrolysable covalent bonds (C=O), the hydrolysis rate depends on parameters such as humidity, temperature, pH and time; therefore, the obtained degradation rate was different for the two used test methods (composting and accelerated weathering). In agreement with previous works (Lucas *et al*. 2008), during composting, the protonation of the hydroxyl end group forms an intramolecular hydrogen bond in the range of pH= 5.5-8.

The hydrolysis of the ester group allows the release of a lactic acid molecule, leading to the decrease in the PLA polymerization degree. The intramolecular random protonation of the carbon belonging to the ester group conduces also to the hydrolysis of ester linkages. This hydrolysis process produces different fragments of lower molecular weight chains, serving as food for bacteria found in the middle of compost. These short chains of PLA weaken the structural resistance of HDPE, generating porosity and void formation in the HDPE/PLA blends, and as a consequence, its degradation rate is increased and affects the mechanical properties. It is well known that the biodegradation of HDPE is difficult because it has a well-organized molecular framework that prevents the diffusion of O_2 and H_2O, starting its degradation within disorganized molecular regions that initially were in lower proportions (Lucas *et al*. 2008).

During the accelerating weathering process, the degradation mechanism starts through PLA photo-oxidation (Bocchini *et al*. 2010). Photodegradation involves anhydride groups, which are easily decomposed in carboxylic acids by hydrolysis corresponding to a Norrish II mechanism of carbonyl polyester (Ikada, 1997), which goes on with HDPE degradation through a Norrish I mechanism. A general scheme of the radical oxidation process of irradiated HDPE/PLA blends is proposed, where the hydroperoxide chain propagation and formation of anhydrides by photolysis of hydroperoxide are indicated.

Bocchini *et al*., (2010) have explained in detail the formation of anhydride groups through a photo-oxidation radical mechanism of PLA with hydroperoxide as intermediary. The photo-oxidation process begins with radicals formed from impurities by UV-irradiation for thermal decomposition. A second step considers the elimination of tertiary hydrogen from the PLA chain to form a tertiary radical (a) which reacts with oxygen to form peroxide (b), which attracts another hydrogen atom from a tertiary

carbon to form hydro-peroxide (c). This intermediary undergoes photolysis (d) obtaining the formation of anhydride groups.

Conclusions

The present study was aimed at increasing the degradation of HDPE by modifying its microstructures with different amounts of PLA by the extrusion process. From the results discussed above, the following conclusions can be drawn: The XRD studies showed that PLA reduced the crystallite size, affecting the known pathways during the HDPE crystallization: a) critical nucleus on the front of the growing spherulite, b) the diffusion in the chain through the matrix of other chains near the growing spherulite, and c) the diffusion of the center of mass of the crystallizable polymer chains in HDPE toward the growing front. The ratio of the viscosities in all the samples was lower than 1 (η_{PLA}/η_{HDPE}=0.01), allowing a coarse droplet morphology. An increase in the roughness with the PLA amount supported the increasing immiscibility of polymer blends.

The immiscible HDPE/PLA blends showed a physical interaction with a reduction in the ordered phase of the HDPE polymer matrix, provoking a reduction of the mechanical properties and an increase in the degradation rate. In the most severe case, the tensile strength could be reduced up to 12.7% in comparison with pure HDPE. A similar trend was obtained during the Izod impact measurements, although in this case, higher PLA quantities (20 wt-%) caused an increase in the break energy due to the brittle nature of PLA. This observation pointed out that a maximum PLA quantity that must be added to the HDPE polymer matrix with a balance between mechanical properties and degradation rate was 15 wt-%. In general, the degradation of HDPE/PLA blends began at PLA sites followed by a subsequent weakening of the chemical structure of HDPE. The degradation mechanism is modified according to the reaction media; with accelerated weathering, it occurred through a photo-oxidation process, whereas hydrolytic degradation was obtained with composting.

A lifetime reduction of about 60% was obtained when the HDPE/PLA blend was prepared with an 85/15 ratio, which also showed a good balance in the mechanical properties and could be considered as an option to be applied in packaging material.

Finally, after degradation, the thermal and mechanical properties were detrimental in comparison with HDPE, corroborating the influence of PLA on the degradation process.

Acknowledgements

Authors wish to thank COFAA-IPN, CONACYT and IPN for scholarship grant and financial support through the Projects, C2014-1905, CB2015-252181, SIP-M2018-1932, SIP2018-1171 and SIP2018-0496. To A. C. Espíndola-Flores for her technical support and Indelpro company for mechanical and MFI tests.

References

Ali Shah A., Hasan F., Hameed A., Ahmed S. (2008). Biological degradation of plastics: A comprehensive review. *Biotechnology Advances 26*, 246-265.

Arjmandi R., Hassan A., Eichhorn S. J., Haafiz M. K. M., Zakaria Z., Tanjung F. A. (2015). Enhanced ductility and tensile properties of hybrid montmorillonite/cellulose nanowhiskers reinforced polylactic acid nanocomposites. *Journal of Materials Science 50*, 3118-3130.

Artham T., Doble M. (2008). Biodegradation of aliphatic and aromatic polycarbonates. *Macromolecular Bioscience 8*, 14-24.

ASTM D1238 (2004). Standard test method for melt flow rates of thermoplastics by extrusion plastometer, active standard. *Annual Book of ASTM Standards, ASTM International*. West Conshohocken, PA.

Bocchini S., Fukushima K., Di Blasio A., Fina A., Frache A., Geobaldo F. (2010). Polylactic acid and polylactic acid-based nanocomposite photooxidation. *Biomacromolecules 11*, 2919-2926.

Chandra R., Rustgi R. (1998). Biodegradable polymers. Progress in Polymer Science 23, 1273-1335. Chen Y., Zou H., Liang M., Cao Y. (2014). Melting and crystallization behavior of partially miscible high density polyethylene/ethylene vinyl acetate copolymer (HDPE/EVA) blends. *Thermochimica Acta 586*, 1-8.

Chouit F., Guellati O., Boukhezar S., Harat A., Guerioune M., Badi N. (2014). Synthesis and characterization of HDPE/N-MWNT nanocomposite films. *Nanoscale Research Letters 9*, 288.

Cuadri A.A., Martín-Alfonso J.E. (2017). The effect of thermal and thermo-oxidative degradation conditions on rheological, chemical and thermal properties of HDPE. *Polymer Degradation and Stability 141*, 11-18.

Dikobe D.G., Luyt A.S. (2017). Thermal and mechanical properties of PP/HDPE/wood powder and MAPP/HDPE/wood powder polymer blend composites. *Thermochimica Acta 654*, 40-50.

Garg S., Jana A. K. (2007). Studies on the properties and characteristics of starch−LDPE blend films using cross-linked, glycerol modified, cross-linked and glycerol modified starch. *European Polymer Journal 43*, 3976-3987.

Gorrasi G., Milone C., Piperopoulos E., Lanza M., Sorrentino A. (2013). Hybrid clay mineral-carbon nanotube-PLA nanocomposite films. Preparation and photodegradation effect on their mechanical, thermal and electrical properties. *Applied Clay Science 71*, 49-54.

Gu J.D., Ford T.E., Mitton D.B., Mitchell R. (2011). Microbial corrosion of metals. In: *Uhlig's Corrosion Handbook*, 3rd. edition, (R. W. Revie ed.), Pp. 421−438. John Wiley & Sons, New York.

Hamad K., Kaseem M., Deri F. (2011). Effect of recycling on rheological and mechanical properties of poly(lactic acid)/polystyrene polymer blend. *Journal of Materials Science 46*, 3013-3019.

Harris M. G., Starita J. M. (2011). *Polyethylene melt blends for high density polyethylene applications*, US 7,867,588 B2, Media Plus Inc.

Heinrich G. (2011). Advanced rubber composites. *Advances in Polymer Science 239*, 1-84.

Huang G., Zou Y., Xiao M., Wang S., Luo W., Han D., Meng Y. (2015). Thermal degradation of poly(lactide-co-propylene carbonate) measured by TG/FTIR and Py-GC/MS. *Polymer Degradation and Stability 117*, 16-21.

Ikada E. (1997). Photo- and Bio- degradable Polyesters. Photodegradation behaviours of aliphatic polyesters. *Journal of Photopolymer Science and Technology 10*, 265-270.

Islam M. Z., Gross B. A., Rowe R. K. (2011). Degradation of exposed LLDPE and HDPE geomembranes: A Review. In: *Geo-Frontiers 2011: Advances in Geotechnical Engineering*, (J. Han, D. E. Alzamora, eds.), Pp. 2065-2072. ASCE, Dallas.

Jabarin S. A., Lofgren E. A. (1994). Photooxidative effects on properties and structure of high density polyethylene. *Journal of Applied Polymer Science 53*, 411-423.

Kaci M., Sadoun T., Cimmino S. (2000). HALS stabilization of LDPE films used in agricultural applications. *Macromolecular Materials and Engineering 278*, 36-42.

Kale G., Auras R., Singh S. P. (2006). Degradation of Commercial Biodegradable Packages under Real Composting and Ambient Exposure Conditions. *Journal of Polymers and the Environment 14*, 317-334.

Kang H., Lu X., Xu Y. (2015). Properties of immiscible and ethylene-butyl acrylate-glycidyl methacrylate terpolymer compatibilized poly (lactic acid) and polypropylene blends. *Polymer Testing 43*, 173-181.

Kawai F. (1995). Breakdown of plastics and polymers by microorganisms. In: *Microbial and Enzymatic Bioproducts, part of the Advances in Biochemical Engineering/Biotechnology 52* (Fiechter, A., ed.), Pp. 151-194. Springer-Verlag Berlin Heidelberg.

Kelly A. L., Brown E. C., Coates P. D. (2006). The effect of screw geometry on melt temperature profile in single screw extrusion. *Polymer engineering and Science 46*, 1706-1714.

Kerry-Rowe R., Sangam H. P. (2002). Durability of HDPE geomembranes. *Geotextiles and Geomembranes 20*, 77-95.

Krässig H. A., Lenz J., Mark H. F. (1984) *Fiber Technology: From film to fiber*. International Fiber Science and Technology Series 4. M. Dekker, New York.

La Mantia F.P., Botta L., Morreale M., Scaffaro R. (2012). Effect of small amounts of poly(lactic acid) on the recycling of poly(ethylene terephthalate) bottles. *Polymer Degradation and Stability 97*, 21-24.

Lee S. I., Chun B. C. (1998). Effect of EGMA content on the tensile and impact properties of poly (phenylene sulfide) EGMA blends. *Polymer 39*, 6441-6447.

Leja K., Lewandowicz G. (2010). Polymer biodegradation and biodegradable polymers – a review. *Polish Journal of Environmental Studies 19*, 255-266.

Leon Janssen P. B. M., Moscicki L. (2009). *Thermoplastic Starch: A Green Material for Various industries*. Editorial Wiley VCH, Verlag, Weinheim.

Loyens W., Groeninckx G. (2002). Ultimate mechanical properties of rubber toughened semicrystalline PET at room temperature. *Polymer 43*, 5679-5691.

Lucas N., Bienaime C., Belloy C., Queneudec M., Silvestre F., Nava-Saucedo J. (2008). Polymer biodegradation: Mechanisms and estimation techniques. *Chemosphere 73*, 429-442.

a Madhu G., Bhunia H., Bajpai P. K. (2014). Blends of high density polyethylene and poly(L-lactic acid): mechanical and thermal properties. *Polymer Engineering Science 54*, 2155-2160.

b Madhu G., Bhunia H., Bajpai P. K., Chaudhary V. (2014). Mechanical and morphological properties of high density polyethylene and polylactide blends. *Journal of Polymer Engineering 34*, 813-821.

Madhu G., Mandal D. K., Bhunia H., Bajpai P. K. (2015). Thermal degradation kinetics and lifetime of high-density polyethylene/poly(L-lactic acid) blends. *Journal of Thermoplastic Composite Materials*, 1-21.

a Madhu G., Mandal D. K., Bhunia H., Bajpai P. K. (2016). Thermal degradation and lifetime of HDPE/PLLA/pro-oxidant blends. *Journal of Polymer Engineering*, 1-15.

b Madhu G., Bhunia H., Bajpai P. K., Nando G. B. (2016). Physico-mechanical properties and biodegradation of oxo-degradable HDPE/PLA blends. *Polymer Science, Series A 58*, 57-75.

Magonov S. N., Cleveland J., Elings V., Denley D., Whangbo M.H. (1997). Tapping-mode atomic force microscopy study of the near-surface composition of a styrene-butadiene-styrene triblock copolymer film. *Surface Science 389*, 201-211.

Martínez-Romo A., González Mota R., Soto Bernal J. J., Frausto Reyes C., Rosales Candelas I. (2015). Effect of ultraviolet radiation in the photo-oxidation of high density polyethylene and biodegradable polyethylene films. *Journal of Physics: Conference Series 582*, 012026.

Meneses J., Corrales C. M., Valencia M. (2007). Síntesis y caracterización de un polímero biodegradable a partir del almidón de yuca. *EIA 8*, 57-67.

Mishra S., Tripathy S.S., Misra M., Mohanty A. K. Nayak S. K. (2002). Novel eco-friendly biocomposites: biofiber reinforced biodegradable polyester amide composites−fabrication and properties evaluation. Journal of Reinforced Plastics and Composites 21, 55-70.

Monticelli O., Calabrese M., Gardella L., Fina A., Gioffredi E. (2014). Silsesquioxanes: Novel compatibilizing agents for tuning the microstructure and properties of PLA/PCL immiscible blends. *European Polymer Journal 58*, 69-78.

Moura I., Machado A. V., Duarte F. M. Nogueira R. (2011). Biodegradability assessment of aliphatic polyesters-based blends using standard methods. *Journal of Applied Polymer Science 119*, 3338-3346.

Muasher M., Sain M. (2006). The efficacy of photostabilizers on the color change of wood filled plastic composites. *Polymer Degradation and Stability 91*, 1156-1165.

Mueller R. J. (2006). Biological degradation of synthetic polyesters−Enzymes as potential catalysts for polyester recycling. *Process Biochemistry 41*, 2124-2128.

Musil J., Zatloukal M. (2011). Experimental investigation of flow induced molecular weight

fractionation during extrusion of HDPE polymer melts. *Chemical Engineering Science 66*, 4814-4823.

Nerkar M., Ramsay J. A., Ramsay B. A., Vasileiou A. A., Kontopoulou M., (2015). Improvements in the melt and solid-state properties of poly(lactic acid), poly-3-hydroxyoctanoate and their blends through reactive modification. *Polymer 64*, 51-61.

Oudhuis A. C. M., Thiewes H. J., van Hutten P. F., ten Brinke G. (1994). A comparison between the morphology of semicrystalline polymer blends of poly(ε-caprolactone)/poly(vinyl methyl ether) and poly(ε-caprolactone)/(styrene-acrylonitrile). *Polymer 35*, 3936-3942.

Parthasarathi V., Sundaresan B., Dhanalakshmi V., Anbarasan R. (2010). Functionalization of HDPE with aminoester and hydroxyester by thermolysis method−An FTIR-RI approach. *Thermochimica Acta 510*, 61-67.

Peng Y., Liu R., Cao J. (2015). Characterization of surface chemistry and crystallization behavior of polypropylene composite reinforced with wood flour, cellulose, and lignin during accelerated weathering. *Applied Surface Science 332*, 253-259.

Petinakis E., Yu L., Simon G., Dean K. (2013). Natural fibre bio-composites incorporating poly(lactic acid). In: *Fiber Reinforced Polymers - the Technology Applied for Concrete Repair* (Masuelli, M. A., ed.), Pp. 41-59. InTech, Rijeka.

Ploypetchara N., Suppakul P., Atong D., Pechyen C. (2014). Blend of polypropylene/poly(lactic acid) for medical packaging application: physicochemical, thermal, mechanical, and barrier properties. *Energy Procedia 56*, 201-210.

Pospisil J., Nespurek S. (1997). Highlights in chemistry and physics of polymer stabilization. *Macromolecular Symposia 115*, 143-163.

Raghavan D., Emekalam A. (2001). Characterization of starch/polyethylene and starch/polyethylene/poly(lactic acid) composites. *Polymer Degradation and Stability 72*, 509-517.

Rundnik E., Briassoulis D. (2011). Comparative biodegradation in soil behavior of two biodegradable polymers based on renewable resources. *Journal of Polymers and the Environment 19*, 18-39.

Scaffaro R., Morreale M., Mirabella F., La Mantia F. P. (2011). Preparation and recycling of plasticized PLA. *Macromolecular Materials and Engineering 296*, 141-150.

Sinclair R. G. (1993). *Blends of polyactic acid*. US5216050 A. Biopaqk Technology, Ltd.

Sinclair R. G., Preston J. (1993). *Degradable impact modified polylactic acid*. US5252642 A, Biopak Technology, Ltd.

Soroudi A., Jakubowicz I. (2013). Recycling of bioplastics, their blends and biocomposites: A review. *European Polymer Journal 49*, 2839-2858.

Stark N. M., Matuana L. M. (2004). Surface chemistry changes of weathered HDPE/wood-flour composites studied by XPS and FTIR spectroscopy. *Polymer Degradation and Stability 86*, 1-9.

Sudhakar M., Sriyutha P., Venkatesan R. (2008). Marine microbe-mediated biodegradation of low and high density polyethylene. *International Biodeterioration and Biodegradation 61*, 203-213.

Temiz A., Terziev N., Eikenes M., Hafren J. (2007). Effect of accelerated weathering on surface chemistry of modified wood. *Applied Surface Science 253*, 5355-5362.

Torres-Huerta A. M., Palma-Ramírez D., Domínguez-Crespo M. A., del Angel-López D., de la Fuente D. (2014). Comparative assessment of miscibility and degradability on PET/PLA and PET/chitosan blends. *European Polymer Journal 61*, 285-299.

van Franeker, J. A., Law, K. L. (2015). Seabirds, gyres and global trends in plastic pollution. *Environmental Pollution 203*, 89-96.

Vera-Sorroche J., Kelly A., Brown E., Coates P., Karnachi N., Harkin-Jones E., Li K., Deng J. (2013) Thermal optimisation of polymer extrusion using in-process monitoring techniques. *Applied Thermal Engineering 53*, 405-413.

Vu B., Chen M., Crawford R. J., Ivanova E. P. (2009). Bacterial extracellular polysaccharides involved in biofilm formation. *Molecules 14*, 2535-2554.

Wang D. K., Varanasi S., Fredericks P. M., Hill D. J.T., Symons A. L., Whittaker A. K., Rasoul F. (2013). FT-IR characterization and hydrolysis of PLA-PEG-PLA based copolyester hydrogels with short PLA segments and a cytocompatibility study. *Journal of Polymer Science Part A: Polymer Chemistry 51*, 5163-5176.

Wang J., Lessard B. H., Maric M., Favis B. D. (2014). Hierarchically porous polymeric materials from ternary polymer blends. *Polymer 55*, 3461-3467.

Wilbrink M. W. L., Argon A. S., Cohen R. E., Weinberg M. (2001). Toughenability of Nylon-6 with $CaCO_3$ filler particles: new findings and general principles. *Polymer 42*, 10155-10180.

Wypych G. (2013). *Handbook of Material Weathering*, ChemTec Pub., Toronto.

Yuan Q., Jiang W., Zhang H., Yin J., An L., Li R. K. Y. (2001). Brittle−ductile transition in high-density polyethylene/ glass-bead blends: effects of interparticle distance and temperature. *Journal of Polymer Science Part B: Polymer Physics 39*, 1855-1859.

Yuan Z. Favis B.D. (2004). Macroporous poly(l-lactide) of controlled pore size derived from the annealing of co-continuous polystyrene/poly(l-lactide) blends. *Biomaterials 25*, 2161-2170.

Zhang M., Zhao B., Liu X. (2015). Predicting industrial polymer melt index via incorporating chaotic characters into Chou's general PseAAC.*Chemometrics and Intelligent Laboratory Systems 146*, 232-240.

Zou H., Yi C., Wang L., Xu W. (2010). Crystallization, hydrolytic degradation, and mechanical properties of poly (trimethylene terephthalate)/poly(lactic acid) blends. *Polymer Bulletin 64*, 471-481.